Oxidation-controlled, Strain-Promoted Tellurophene-Alkyne Cycloaddition (OSTAC): A Bioorthogonal Reaction for Fast and Selective Protein Conjugation

Yong Jia Bu[a] and Mark Nitz*[a]
[a]Department of Chemistry, University of Toronto 80 St. George Street, Toronto, ON, M5S3H6, Canada
mark.nitz@utoronto.ca

Abstract

Noncanonical amino acids (ncAAs) bearing functional groups for bioorthogonal labelling are useful tools for the downstream analysis of nascent polypeptides. However, the methionine analogues commonly used are not optimally recognized by the endogenous protein synthesis machinery. TePhe, a tellurophene bearing phenylalanine analogue, is a promising alternative to the methionine analogues as it is readily accepted, and incorporated, during protein synthesis. However, a bioorthogonal reaction to label TePhe was required to enable protein tagging to facilitate analysis. Here we establish that the tellurophene side chain of TePhe is a potent partner in an oxidation-controlled, strain-promoted tellurophene-alkyne cycloaddition (OSTAC) reaction. Mild oxidation of the tellurophene ring with *N*-chlorosuccinimide produces a Te(IV) species which undergoes rapid (k > 100 $M^{-1}s^{-1}$) cycloaddition with bicyclo[6.1.0]nonyne (BCN) resulting in a benzo-fused cyclooctane. Selective reaction of TePhe containing proteins can be achieved in complex protein mixtures. OSTAC reactions can be combined with strain-promoted azide alkyne cycloaddition (SPAAC) and copper catalyzed azide alkyne click (CuAAC) reactions. The favorable properties of the OSTAC reaction will likely find wide application beyond its use with TePhe in chemical biology.

Introduction

Strict control of protein synthesis is critical to proper cellular function, while aberrant expression leads to toxicity and disease.[1-3] The ability to characterize proteomic changes in response to environmental and physiological signals is key to addressing many questions in biology and medicine. Although many methodologies have been developed to track translation and to identify nascent proteins[4-7], these experiments remain non-trivial. We previously developed L-tellurienylalanine (TePhe, Fig. 1), a tellurium (Te)-containing analogue of phenylalanine (Phe), for tracking active translation through metabolic incorporation into proteins and detection of Te by mass cytometry (MC).[8] This strategy is effective for determination of global protein synthesis levels, but provides no protein-specific information due to the complete atomization of biomolecules during MC measurements. Consequently, we sought to develop a tellurophene-specific bioorthogonal reaction as a means of labeling TePhe-containing proteins for downstream analysis. Such a method would provide sequence-specific information directly complementary to aggregated data generated by MC and expand the available toolbox for interrogating proteome dynamics. Furthermore, a tellurophene-based bioorthogonal reaction could be used more broadly to complement the other powerful bioorthogonal reactions available for chemical biology.[9-12]

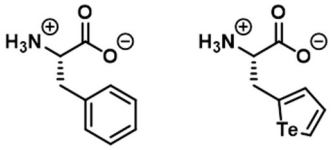

Figure 1. Structures of L-phenylalanine (Phe) and L-tellurienylalanine (TePhe).

Existing methods for the labeling and capture of newly synthesized proteins include bioorthogonal non-canonical amino acid tagging (BONCAT)[13], recoding by genetically engineered aminoacyl-tRNA synthetases[14,15], and puromycinylation of nascent peptides.[16-18] Each strategy is associated with unique advantages and drawbacks. BONCAT relies on the metabolic incorporation of methionine (Met) analogues, homopropargylglycine (HPG) and azidohomoalanine (AHA), for downstream click chemistry; the procedure is easy to perform but often requires amino acid depletion and high concentrations of probe due to low affinity of Met-tRNA synthetase for HPG/AHA.[19] Genetic engineering approaches offer better incorporation efficiency but have an inherently higher barrier to application. Puromycinylation can provide an instantaneous snapshot of active translation, but generates truncated peptides and is not always a reliable reporter of protein synthesis.[20,21] In contrast, TePhe displays robust metabolic labeling at low concentrations in both minimal and rich media[8], does not require specially engineered aminoacylation machinery, and preserves protein length, structure, and stability due to its high isosterism to Phe.[22,23] Pending the development of a tellurophene-specific reaction, TePhe could be used in a BONCAT approach, but with potential advantages of higher

incorporation efficiency and greater sequence coverage by virtue of the greater frequency of Phe than Met across the proteome.[24]

The Seferos group established that strong oxidants such as halogens and peroxides readily oxidize π–extended tellurophenes at the Te centre[25-27], and that the reaction can take place in water as well as in organic solvents.[28] The oxidized tellurophene has reduced aromatic character compared to the parent compound[25], which we considered a promising starting point to increase the reactivity of the tellurophene. In contrast to the π–extended tellurophenes, oxidized TePhe revealed a propensity to engage in cycloaddition reactions with itself and other partners. Herein, we describe the oxidation of TePhe under mild conditions. The Te(IV) species undergoes a selective [4+2] cycloaddition with the strained alkyne bicyclo[6.1.0]nonyne (BCN). The reaction proceeds cleanly in the context of peptides, purified proteins, and cell lysates. Furthermore, the reaction is rapid with second order rate constants of ~100 $M^{-1}s^{-1}$ and can be used in combination with strain promoted azide alkyne cycloaddition (SPAAC) and copper catalyzed azide alkyne click (CuAAC). We demonstrate that small quantities of TePhe-containing proteins can be readily labeled within complex proteomic mixtures, representing significant progress towards the goal of using TePhe as a mediator of nascent protein capture.

Results and Discussion

Oxidized Tellurophenes participate in cycloaddition reactions.

N-acetyl-L-TePhe-isopropylamide (Ac-TePhe-*i*Pr, **1**) was used to characterize TePhe reactivity in aqueous media. In phosphate-buffered saline (PBS), *N*-chlorosuccinimide (NCS)—a mild, water-soluble, and shelf-stable oxidant—readily oxidizes the Te centre of the TePhe side chain from the Te(II) to Te(IV) state, as indicated by the upfield shift of tellurophene proton resonances reflecting decreased aromatic character upon oxidation[25] (Fig S1, S2). Water solubility of the tellurophene increases significantly upon oxidation, consistent with observations made for the analogous oxidation of selenophenes[29] and of tellurapyrylium dyes.[30] In aqueous buffer, the Te(IV) tellurophene **2** likely exists as a rapid equilibrium between a number of species, including the telluroxide[31], its hydrated form and associated protonation states[30,32,33], and possibly halide- or other anion-coordinated Te(IV), as seen by ESI-MS (Fig. S3). NCS does not appear to oxidize the tellurophene side chain past the Te(IV) state, however, the use of a stronger oxidant, H_2O_2, slowly produces more upfield resonances presumed to belong to the completely de-aromatized Te(VI) ring (Fig. S1) which are not observed when using NCS.

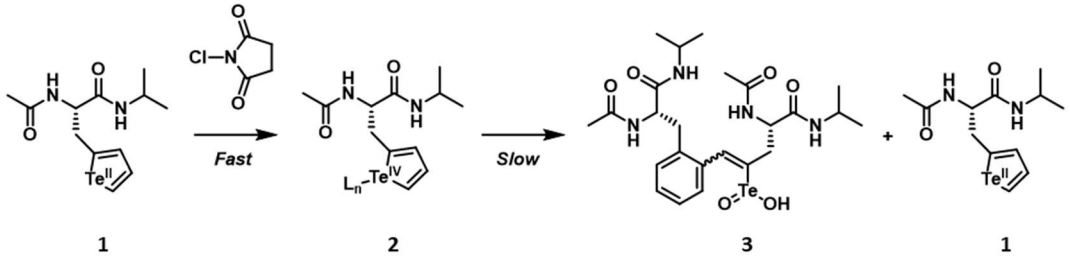

Figure 2. Ac-Te^{II}Phe-*i*Pr is oxidized by NCS to Ac-Te^{IV}Phe-*i*Pr and slowly undergoes a cycloaddition reaction.

Ac-Te^{IV}Phe-*i*Pr (**2**) is moderately stable in solution. Following ^{1}H NMR spectra of **2** in aqueous buffer over the course of two days showed the gradual disappearance of oxidized tellurophene, re-emergence of the unoxidized starting material and a new species that likely arises from the dimerization of **2** (Fig. S2), as is observed with oxidized thiophenes.[34-36] The structure of the product **3** was inferred from ESI-MS and NMR characterization (Fig S2, S4). The rate of oxidized tellurophene consumption determined by ^{1}H NMR is consistent with a second order reaction (k_{obs} 0.02 M^{-1} s^{-1}, Fig. S5). Due to challenges in isolating and characterizing the dimerization product **3**, we explored trapping the oxidized tellurophene **2** with an alternative cycloaddition partner to verify the reactivity of **2** as a diene. *N*-methylmaleimide provided telling results, forming three distinct products (Fig. S6a, S6b) consistent with **2** being a potent diene: a non-aromatic single cycloadduct, an aromatized single cycloadduct, and a non-aromatic double cycloadduct. To simplify the cycloaddition of oxidized tellurophenes we chose to explore strained alkynes, which should be sufficiently reactive to outcompete dimerization, and upon extrusion of tellurium, generate a single aromatic product.

Reaction of oxidized Ac-TePhe-*i*Pr with strained alkynes.

Cyclooctyne and bicyclo[6.1.0]nonyne (BCN) derivatives have been used as dienophiles in [4+2] cycloaddition with oxidized thiophenes[37-39] (Fig. 3a). The reactions require either electron-withdrawing substituents

on the thiophene ring[37,38] or heating and long reaction times.[39] Furthermore, these reactions require formation of the oxidized species prior to introduction of the strained alkyne. We were delighted to find that *in situ* oxidation of Ac-Te^{II}Phe-*i*Pr (**1**) with NCS (3 eqv.) in the presence of *endo*-bicyclo[6.1.0]non-4-yn-9-yl methanol (*endo*-BCN-OH) rapidly and cleanly forms the desired benzocyclooctane product **4** under ambient conditions. Analysis of the reaction by ^{1}H NMR indicated complete conversion to a new multiplet at 7.0 ppm, with no evidence of any reversion to Te(II) tellurophene or dimer formation (Fig. 3c. Fig. S7a, S7b). The progress of this oxidation-controlled, strain-promoted tellurophene-alkyne cycloaddition (OSTAC) reaction was too rapid to monitor by NMR spectroscopy, but could be tracked using the weak absorption band of **2** at 323 nm (Fig. 3d). The initial oxidation of Ac-Te^{II}Phe-*i*Pr (**1**) to Ac-Te^{IV}Phe-*i*Pr (**2**) by NCS is extremely rapid and thus excluded from our analysis; this is in line with reports that the kinetics of oxidation of certain Te(II) heterocycles by halogens approach the diffusion limit.[40] At low-micromolar concentrations of reactants, the cycloaddition of **2** and *endo*-BCN-OH is complete within 20 minutes, with a 2nd order rate constant of 109 ± 10 $M^{-1}\cdot s^{-1}$ with 2.5 eqv. NCS to **1** (Fig. 3e, S8a). Increasing the excess of NCS did not alter the measured rate constant (120 ± 10 $M^{-1}\cdot s^{-1}$ and 110 ± 10 $M^{-1}\cdot s^{-1}$ at 4 and 8 eqv. NCS respectively, Fig. S8b), suggesting that cycloaddition rather than the oxidation steps is rate-limiting. This relatively large rate constant makes the desired cycloaddition with *endo*-BCN-OH over 5000 times faster than dimerization. The OSTAC reaction is also significantly faster than most azide (SPAAC) or nitrone additions (SPANC) to strained alkynes[41], and is on par with that of the copper-catalyzed azide-alkyne click (CuAAC) reaction.[42,43]

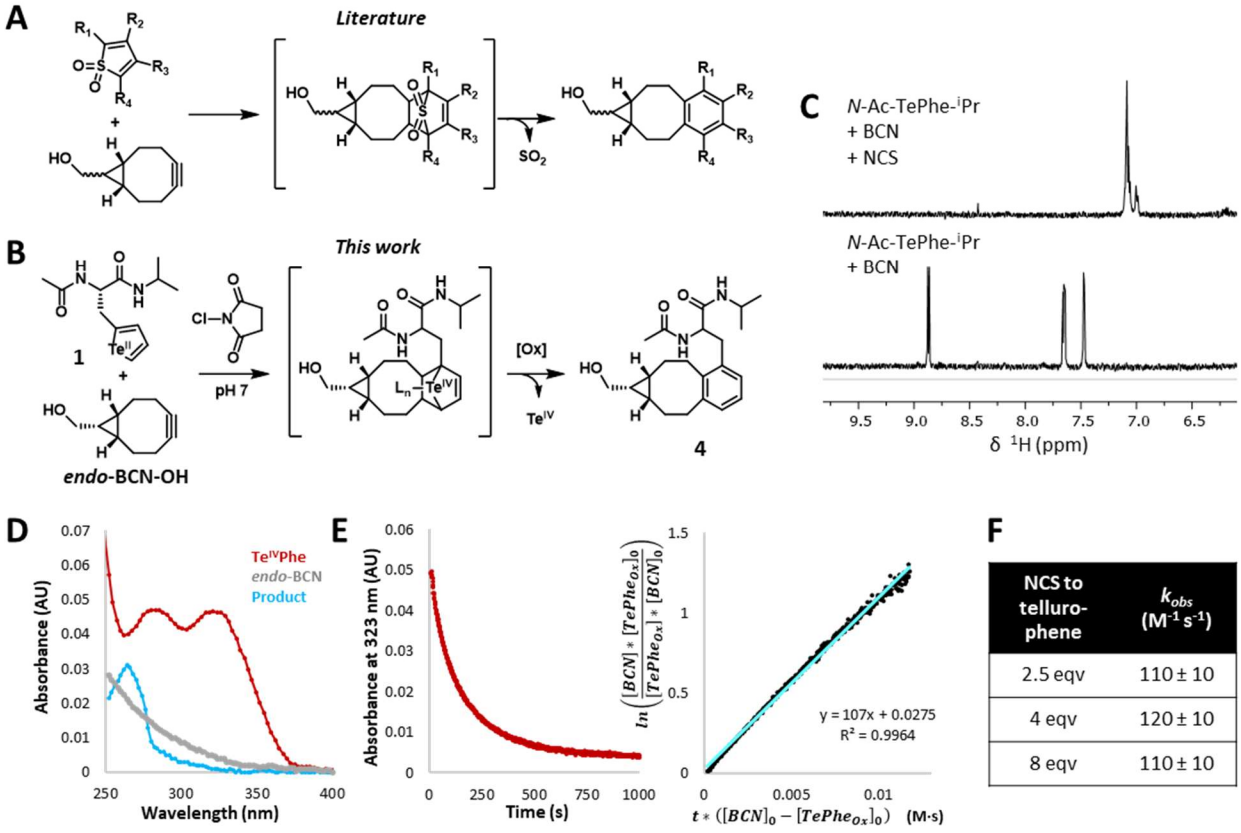

NCS to telluro-phene	k_{obs} ($M^{-1}s^{-1}$)
2.5 eqv	110 ± 10
4 eqv	120 ± 10
8 eqv	110 ± 10

Figure 3. Cycloaddition of oxidized TePhe with BCN. A) Literature reactions of thiophene 1,1-dioxides with BCN. B) OSTAC reaction between **1** and BCN C) Reaction of Ac-TePhe-*i*Pr (**2**, 2 mM) with *endo*-BCN-OH (4 mM) with or without NCS (6 mM) in phosphate buffer (50 mM, pD 7.4, 10% MeOD) as monitored by NMR spectroscopy (^{1}H, 500 MHz, 298 K) 15 min after NCS addition. D) UV-visible absorbance spectra of **2** (50 μM), *endo*-BCN-OH (80 μM), and cycloadduct (80 μM) in phosphate buffer (2 mM, pH 7), 5% D_2O, 10 % MeOH in H_2O. E) Kinetics of reaction of **2** (50 μM) with *endo*-BCN-OH (75 μM) in presence of NCS (125 μM total) as monitored by UV-vis spectrophotometry in PBS. F) Observed rate constants of the OSTAC reaction at varying excesses of NCS indicate no rate dependence on oxidant concentration.

We also attempted to replace BCN with dibenzoazacyclooctyne (DIBAC) as a dienophile in the OSTAC reaction, but found markedly poorer reactivity. The reaction of **2** (1 mM) with DIBAC-Peg_4-hydroxyl (DIBAC-OH, 2 mM) was sufficiently slow to be monitored by ^{1}H NMR spectroscopy, with an estimated maximum rate constant of 0.07 $M^{-1}s^{-1}$ based on disappearance of **2** (Fig. S9a, S9b). OSTAC using DIBAC is therefore at least 3 orders of magnitude slower than with BCN, and falls into a similar kinetic regime as dimerization of **2**. Preference for BCN over DIBAC has been reported for various electron-deficient cycloaddition partners, such as aromatic azides[44], 1,2,4,5-tetrazines[45], and *ortho*-quinones[46].

Reaction of oxidized TePhe and BCN on peptides and proteins.

To evaluate the bio-orthogonality of the OSTAC reaction, we began with the labeling of TePhe-bearing ribonuclease S-peptide which was previously synthesized in our laboratory.[23] Incubation of TePhe S-peptide with BCN and NCS for 30 min at room temperature in PBS showed clean conversion to the desired product by MALDI-MS (Fig. 4a). The distinctive isotopic envelope corresponding to the TePhe containing S-peptide is lost in the presence of BCN and NCS, confirming loss of tellurium from the product.

Encouraged by this result, we expressed three proteins, in the presence of TePhe, with different secondary structural elements and amino acid compositions to be used as labeling targets: *E. coli* maltose binding protein (MBP), *Bacillus circulans* xylanase (Bcx), and Sars-CoV-2 3-chymotrypsin-like protease ($3CL^{pro}$). Recombinant expression in *E. coli* produces heterogeneous ensembles of partially TePhe-substituted proteins[22], which exhibit species separated by approximately 102 Da in the mass spectrum for each Phe to TePhe substitution within a single polypeptide (Figure 4b). The purified protein ensembles were then labeled using NCS and a fluorophore-conjugated BCN probe for visualization by in-gel fluorescence. Due to the nature of NCS as a halogenating agent, the cyanine family of fluorophores are incompatible with our labeling strategy as chlorination of their bridging methines lead to quenching of fluorescence.[47] Fluorescein and rhodamine derivatives are unaffected by NCS, and as such *exo*-BCN-Peg_3-fluorescein (BCN-FAM, Fig. 4c) became our probe of choice for labeling experiments.

MBP, which contains all proteinogenic AAs except cysteine, was used to gauge the efficiency of the OSTAC reaction in the absence of complications from thiol oxidation. Wildtype (Wt, non-TePhe-containing) and TePhe-MBP were incubated with BCN-FAM and increasing concentrations of NCS in phosphate buffer at pH 7 with SDS to denature MBP and reveal the buried TePhe residues. We observed robust FAM labeling that is both TePhe- and oxidation-dependent by SDS-PAGE (Figure 4d, top). A decrease in electrophoretic mobility is observed for all Wt and TePhe-MBP bands treated with NCS, which can be explained by methionine oxidation (thioether to sulfoxide, Fig. S10) observed in ESI-MS analysis of treated proteins. In contrast, only TePhe-MBP bands with extensive labeling by BCN-FAM are broadened, reflecting increased separation of MBP molecules with different levels of TePhe incorporation. ESI-MS analysis of the labeled protein was consistent with selective reaction at TePhe residues (Fig. S10). We also investigated the labeling kinetics of TePhe-MBP by quenching the reaction using an excess of non-fluorescent BCN at desired timepoints. To our surprise, at low concentrations of MBP (0.02 mg/mL, ~500 nM protein) and BCN-FAM (20 μM), the maximum labeling fluorescence is reached in ~5 min (Fig. S11). This is faster than expected based on the small molecule kinetic experiments shown in Fig. 3d and may be due to the effective concentration of protein and probe within SDS micelles.

Other oxidants which have been reported for modifying proteins, such as periodate[46,48-50], did not produce as favourable results as NCS. Labeling MBP with $NaIO_4$ revealed that a 10-fold greater oxidant concentration is needed to achieve labeling levels comparable to NCS, at which point non-specific labeling on Wt MBP becomes extensive (Fig. 4d, bottom). These results suggest that NCS reacts much more quickly with TePhe than $NaIO_4$ while sparing the majority of canonical residues.

Next, we applied the OSTAC reaction to Bcx, which like MBP contains all AAs except for cysteine. We observed similar results, with TePhe- and oxidation-dependent labeling in (Fig. 4e) in minutes. Interestingly, species with different numbers of BCN adducts could be resolved as separate bands on SDS-PAGE, likely due to the relatively small size of Bcx (~20 kDa), making each cycloaddition significantly alter migration.

Finally, $3CL^{pro}$, which contains 12 free cysteine residues, was investigated as a OSTAC target. In addition to consuming NCS, cysteines pose the problem of potential non-specific labeling through thiol-yne reactions with the BCN probe.[51] Wt $3CL^{pro}$ shows a greater amount of BCN-FAM labeling in the presence of NCS than in its absence (Fig. 4f). The nature of this labeling is not clear; it is plausible that NCS is initiating radical processes and promoting thiol-alkyne coupling. The non-specific labeling can be somewhat attenuated through the alkylation of free thiols using iodoacetamide (IAA) prior to addition of NCS and BCN-FAM, suggesting that reduced cysteine side chains at least partially contribute to non-specific labeling. Robust labeling of TePhe $3CL^{pro}$ can still be achieved but additional oxidant is required.

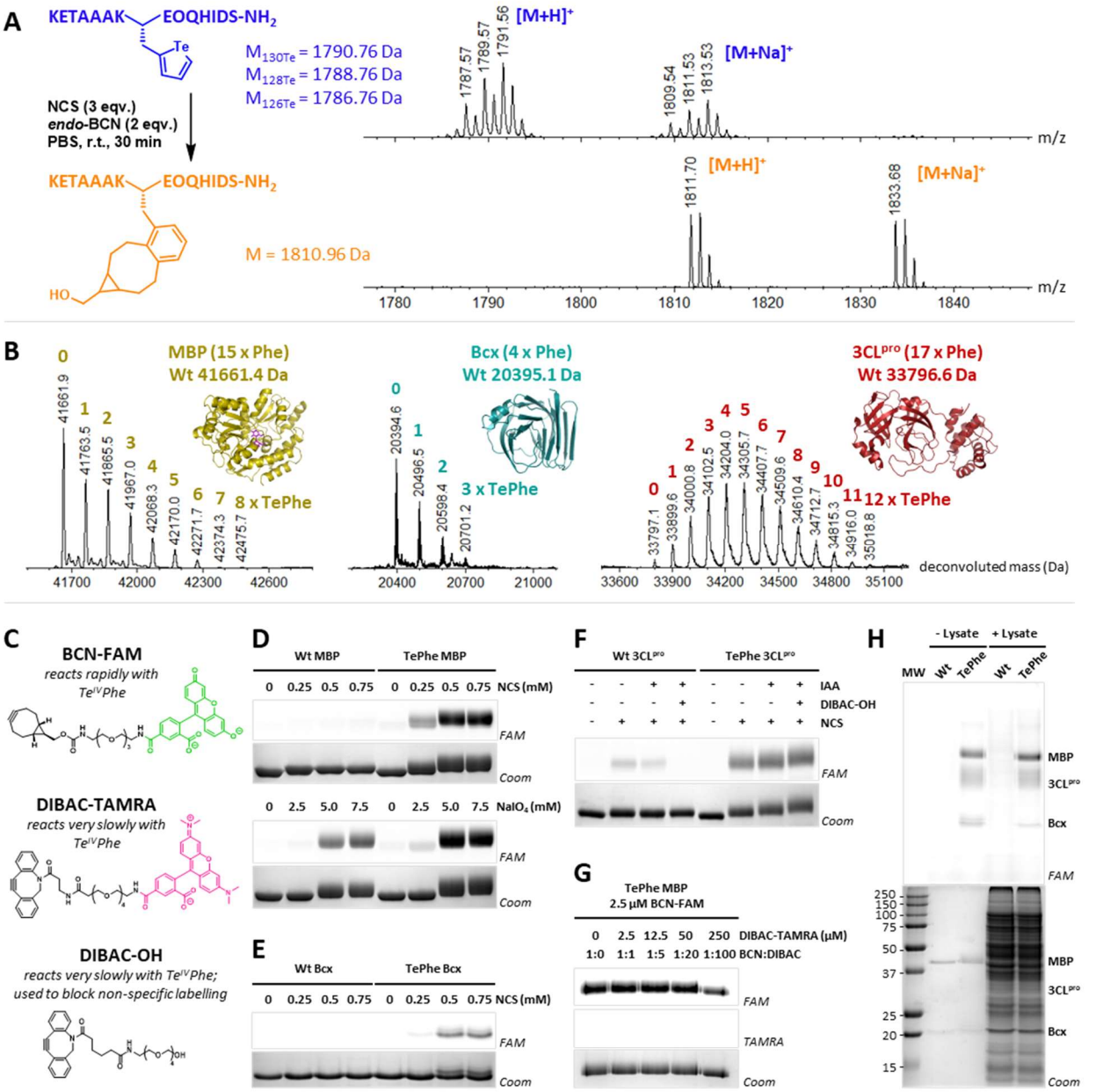

Figure 3. OSTAC in biological samples. A) MALDI-MS analysis of OSTAC reaction between TePhe S-peptide (0.5 mM) and BCN (1 mM) in presence of NCS (1.5 mM) in PBS. B) ESI-MS analyses of TePhe-containing ensembles of maltose binding protein (MBP; PDB ID: 1ANF[53]), *Bacillus circulans* xylanase (Bcx; PDB ID: 1BCX[54]) and Sars-CoV-2 3CL protease ($3CL^{pro}$; fPDB 1D: 7JST[55]), showing varying numbers of Phe→TePhe substitutions per polypeptide. C) Structures of fluorophores and blocking agents used for OSTAC labeling of proteins. D) NCS (top) and $NaIO_4$ (bottom) concentration dependence of OSTAC labeling on Wt and TePhe MBP (1 mg/mL protein, 100 µM BCN-FAM in PBS + 0.2% SDS). E) NCS concentration dependence of OSTAC labeling on Wt and TePhe Bcx (1 mg/mL protein, 100 µM BCN-FAM in PBS + 0.2% SDS). F) Effects of iodoacetamide (IAA, 1 mM, 20 min) and DIBAC (50 µM, 5 min) blocking on OSTAC labeling of Wt and TePhe $3CL^{pro}$ (0.5 mg/mL protein, 100 µM BCN-FAM, 500 µM NCS in PBS + 0.2% SDS). G) Competition of BCN-FAM (2.5 µM) and DIBAC-TAMRA (0 to 250 µM) in the OSTAC reaction for oxidized TePhes on MBP (0.025 mg/ml protein, 20 µM NCS in PBS + 0.2% SDS). H) OSTAC labeling for selective visualization of TePhe MBP, Bcx, and $3CL^{pro}$ (0.01 mg/L) within a non-TePhe-containing proteome (1 mg/mL); IAA (5 mM, 20 min), followed by NCS (200 µM) and DIBAC-OH (50 µM) blocking for 5 min, and finally NCS (100 µM) and BCN-FAM (25 µM) labeling for 5 min.

To eliminate non-specific labeling on Wt 3CL^{pro}, we exploited our findings of low reactivity between **2** and DIBAC. We hypothesized that sites responsible for the observed non-specific reactivity could be capped through the addition of a non-fluorescent DIBAC moiety (DIBAC-OH, Fig. 4c) in the presence of NCS prior to BCN-FAM labeling. To confirm the differential selectivity of these strained alkynes a competition experiment between BCN-FAM and DIBAC-Peg$_4$-tetramethylrhodamine (DIBAC-TAMRA, Fig. 4c) for reaction with oxidized TePhe residues in MBP was carried out, which showed exclusive labeling by BCN-FAM at the maximum (100-fold) excess of DIBAC-TAMRA over BCN-FAM tested (Fig. 4g). Satisfied that DIBAC reacts slowly with TePhe containing proteins, we employed a blocking step by incubation with DIBAC and NCS prior to BCN-FAM labeling (Fig 4f). When used in conjunction with thiol alkylation by IAA, this approach effectively eliminates non-specific ligations without diminishing TePhe labeling, as demonstrated by the difference in fluorescence of the Wt and TePhe-3CL^{pro} bands under this blocking regime (Fig. 4f, 4th and 8th lanes from left; Fig. S12).

Using the conditions optimized above, we tested the selectively of the OSTAC reaction in a cell lysate spiked with TePhe labeled proteins. TePhe-MBP, TePhe-Bcx, and TePhe-3CL^{pro} were each added to *E. coli* lysate at 1% the total protein content, (Fig. 4h; note bands of the proteins of interest are extremely faint and non-discernible within lysate by Coomassie staining). The mixture was alkylated (IAA), blocked with DIBAC-OH and finally labeled with BCN-FAM. By fluorescence, the lysate lanes containing spiked Wt and TePhe proteins effectively mirror their control lanes which contain the same quantities of isolated MBP, Bcx, and 3CL^{pro}, with minimal background labeling and nearly identical labeling efficiency for TePhe proteins in the presence or absence of lysate. The method of blocking non-specific reactivity with DIBAC is generalizable to the proteome, which will allow small amounts of TePhe proteins to be successfully "fished" from a complex mixture.

In addition to suppression of labeling of non-TePhe residues by BCN, we also considered the possibility that the oxidative conditions used in our reaction may promote the formation of covalent crosslinks either between a TePhe and a canonical AA, or between two canonical AAs, which cannot be broken through addition of reducing agent post-labeling. Such crosslinks, if formed intermolecularly, could introduce false positives in pulldown/ enrichment-type experiments where an affinity tag is intended to capture exclusively TePhe-containing proteins. We found no evidence of such inter-protein crosslinking when labeling MBP or Bcx, which were performed at a relatively high concentration of 1 mg/mL protein (Fig. S13a-b). A small amount (≤4% by Coomassie staining) of protein dimer was observed for both Wt and TePhe 3CL^{pro} at 0.5 mg/mL (Fig. S13c). As such, we subjected pairwise mixtures of 3CL^{pro} with Wt BSA, MBP, and Bcx to our labeling conditions to search for crosslinks between 3CL^{pro} and other proteins, but were unable to detect any heterodimer formation (Fig. S14). This suggests that the trace dimerization observed for 3CL^{pro} is most likely a feature of this specific protein rather than a general consequence of our labeling conditions, and should not pose a significant challenge for downstream experiments.

Orthogonality of OSTAC to Azide Alkyne Click Chemistries.

As azides are established bio-orthogonal partners to alkynes, we wished to develop a system where azides and TePhe residues could be orthogonally labeled, such that both moieties may be simultaneously incorporated into a single biological sample for the tracking of different processes. We have already demonstrated that Te^{IV}Phe reacts selectively with BCN over DIBAC, while aliphatic azides are known to have a modest preference for DIBAC over BCN.[52] Non-thiol-containing proteins can be simultaneously subjected to OSTAC and SPAAC chemistry with good selectivity, although the use of excess DIBAC reagent to favour azide-DIBAC over azide-BCN cycloaddition is required (Fig 5a). Using this strategy, we were able to achieve nearly mutually exclusive labeling on a mixture of TePhe MBP (by BCN-FAM) and azidoacetylated BSA (by DIBAC-TAMRA). In mixtures containing thiol-bearing proteins, a sequential reaction which carries out DIBAC-SPAAC prior to OSTAC chemistry would be required, such that the DIBAC probe used for SPAAC can be removed and an untagged DIBAC introduced for the blocking step outlined above. Similarly, we found that the CuAAC and OSTAC reactions can be carried out in a sequential manner without adversely affecting TePhe labeling (Fig 5c). The combination of CuAAC and OSTAC requires stepwise labeling as the use of ascorbate as a reducing agent in CuAAC and need for oxidant to activate TePhe for OSTAC prevents simultaneous reaction. Azidoacetylated BSA (Az-BSA) was first labeled using terminal alkyne-Peg$_4$-TAMRA (Alkyne-TAMRA, Fig. 5b) in the presence or absence of Wt or TePhe-MBP, TePhe-Bcx, and TePhe-3CL^{pro} under denaturing conditions (0.2% SDS). Az-BSA shows similar levels of labeling by alkyne-TAMRA when alone and when in the presence of Wt or TePhe containing proteins (Fig. 5c, "CuAAC only" lanes), suggesting that TePhe does not significantly interfere with CuAAC efficiency. Post-CuAAC, the protein mixtures were buffer-exchanged to remove copper catalyst and reducing agent, and then subjected to NCS oxidation, DIBAC blocking, and reaction with BCN-FAM. TePhe containing proteins displayed BCN-FAM labeling of comparable intensity to a control sample not subjected to CuAAC (Fig. 5c, "CuAAC followed by TePhe-BCN conjugation" lanes), indicating that even when solvent-exposed, TePhe side chains are resilient to CuAAC conditions. In a hypothetical experiment where the

CuAAC step may be performed without denaturant, the majority of TePhe residues are expected to be buried within folded proteins, and are therefore even better protected from oxidative damage that may be caused by the copper catalyst. The above results point to TePhe being suitable for multiplexing alongside azide and unstrained alkyne probes.

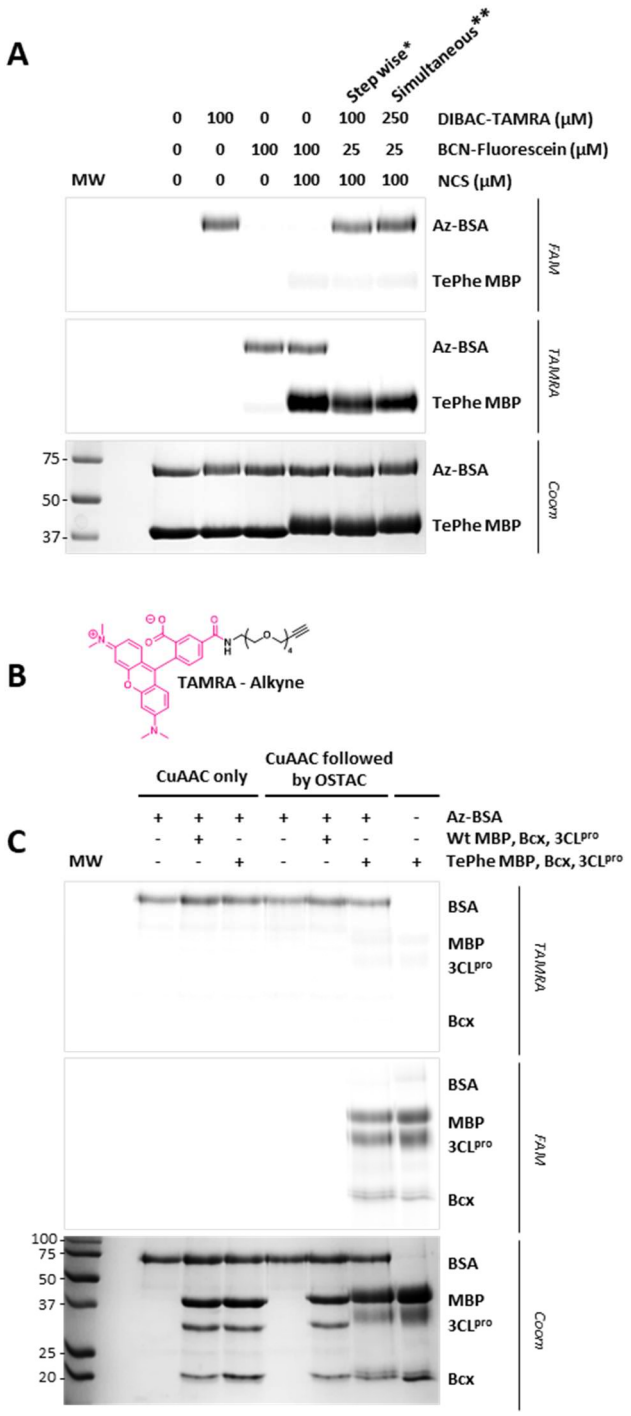

Figure 5. Orthogonality of OSTAC and CuAAC chemistries. A) Orthogonality of SPAAC and OSTAC reactions. Note: TAMRA channel has minor FAM spillover with available filter set, as seen in lane 5. All reactions performed with Az-BSA and TePhe MBP (0.5 mg/mL each) in PBS + 0.2% SDS. B) Structure of terminal alkyne-TAMRA probe used for CuAAC. C) Comparison of CuAAC efficiency on azidoacetylated BSA in the presence and absence of TePhe, and of OSTAC efficiency post-CuAAC.

Conclusion

We describe a tellurophene-specific bioorthogonal ligation reaction which uses commercially available reagents and mild reaction conditions. Encouraged by the robust performance of the OSTAC reaction for fluorescent labeling in complex biological samples, we are now actively working to adapt existing OSTAC procedures for affinity tagging, bringing us closer to the goal of using TePhe as a tool for labeling and capturing nascent proteomes. Perhaps more importantly, the newly discovered tellurophene reactivity opens doors for the development of tellurophene-based probes for other biological processes or bioconjugations that can use this potent bioorthogonal reaction.

Methods

Materials and instrumentation. Reagents for synthesis were purchased from either Millipore Sigma or Chem Impex. Buffers salts, media components, antibiotics, gel electrophoresis reagents, and other materials required for protein expression and purification were purchased from BioShop, Bio-Rad or Sigma. *Endo*-BCN-OH was purchased from Sigma while all other strained alkynes and strained alkyne-fluorophore conjugates were purchased from Click Chemistry Tools. All materials were used as received without further purification. No unexpected or unusually high safety hazards were encountered during synthesis or when performing OSTAC reactions. NMR spectra were acquired on 500 MHz Agilent DD2 spectrometers with either an XSens C13 cold probe or dual resonance OneNMR probe, or 600 MHz Agilent DD2 spectrometer with a triple resonance HFX probe. Small molecule and protein electrospray ionization mass spectra were acquired on an Agilent 6538 UHD Q-TOF mass spectrometer. In-gel fluorescence imaging was performed on a Syngene G:Box Chemi XT 4 gel documentation system.

Synthesis of Ac-TePhe-^{i}Pr (1). This compound was synthesized in 4 steps from L-propargylglycine by adaptation of existing protocols.[8,22] Detailed procedures and spectra can be found in the Supporting Information.

General considerations for oxidation and cycloaddition reactions. Stock solutions of **1** were prepared in D_2O or deuterated PBS and quantitated using DSS as a standard by ^{1}H NMR spectroscopy. **1** has limited water solubility (up to ~2.5 mM) and requires sonication for full dissolution. Once prepared the solutions could be repeatedly frozen and thawed without detectable degradation based on ^{1}H NMR spectroscopy. NCS stock solutions in D_2O (up to 55 mM) were prepared fresh prior to each experiment and also required sonication to aid dissolution. Concentrated buffer stocks were prepared from either loose salts or PBS tablets at 10x or greater. Dienophiles (NMM, BCN, DIBAC) were added to their respective reactions as solids if sufficient mass was used, or as concentrated stock solutions in methanol. Appropriate quantities of the reaction components were delivered by micropipette. NCS was typically added last to begin the reaction.

Oxidation and self-reaction of 1. A solution of **1** (2 mM) and NCS (4 mM) was prepared in deuterated PBS and left to react at room temp. for 2 days. For characterization of Ac-Te^{IV}Phe-^{i}Pr (**2**), reactions were set up in the same manner but in pure H_2O or D_2O without addition of base or buffer.

Attempted isolation of Ac-Te^{IV}Phe-^{i}Pr dimerization product (3). 1 (43 mg, 0.12 mmol, 1 eqv.) was suspended in 100 mM phosphate buffer, pH 7.5 (12 mL), and dissolved by addition of NCS (50 mg, 0.37 mmol, 3 eqv.) to generate a 10 mM solution of oxidized tellurophene **2**. The reaction was left at room temp. for 3 days, after which the mixture was flash-frozen, lyophilized, and resuspended in MeOH to precipitate out salts. Preparatory thin layer chromatography was performed on silica gel 60G F_{254} (30% H_2O/MeOH, product R_f ~0.4-0.5 streaky). Silica harbouring product was removed, sonicated in 10 mL 1:2 MeOH/H_2O, and centrifuged at 21.1 x *g* to obtain a clear aqueous solution, which was lyophilized to yield a solid consisting mostly of dimer and small amounts of NCS-derived impurities. ^{1}H NMR (500 MHz, D_2O, 298 K) δ 7.74 and 7.72 (1H, 2 s, vinyl H), 7.54-7.18 (4H, m, aryl H), 4.48 (1H, 2 overlapping t, J = 6.4 Hz, Hα), 4.38 (1H, 2 overlapping t, J = 8.0 Hz, Hα′), 3.93 (1H, 2 overlapping hept., J = 6.6 Hz, ^{i}Pr-C**H**$(CH_3)_2$), 3.75 (1H, 2 overlapping hept., J = 6.6 Hz, ^{i}Pr′-C**H**$(CH_3)_2$), 3.33-2.91 (4H, m, Hβ), 2.05, 2.04, 1.98, and 1.95 (6 H, 4 s, *N*-Ac-C**H$_3$**), 1.22-0.69 (12H, m, ^{i}Pr-CH(C**H$_3$**)$_2$). ^{13}C NMR (125 MHz, D_2O, 298 K) δ 174.07, 174.01, 173.59, 173.47, 171.65, 171.43, 171.10, 150.90, 141.18, 135.39, 135.29, 131.00, 130.95, 129.97, 129.48, 129.40, 127.87, 54.20, 53.81, 53.55, 41.96, 41.58, 41.54, 35.19, 34.95, 32.86, 32.30, 21.75, 21.69, 21.62, 21.57, 21.32, 21.31, 21.26, 21.23, 21.07, 21.05. Large number of peaks are a result of *cis-trans* isomers and varying conformations for each species.

Reaction of 2 with *N*-methylmaleimide (NMM). A solution of **1** (2.2 mM), NMM (4.5 mM) and NCS (4.5 mM) was prepared in deuterated PBS and heated at 40 °C for 10 hr. Aliquots were removed at 45 min, 2 hr, 4 hr, and 10 hr timepoints (NMR spectra acquired at room temp). Formation of hypothesized cycloadducts was supported by ESI-MS analysis (Fig. S5b).

Reaction of 2 with *endo*-BCN-OH. 1 A solution of **1** (2.0 mM), *endo*-BCN-OH (4 mM), and NCS (6 mM) was prepared in 50 mM phosphate buffer, pD 7.4 in D_2O + 10% MeOD + DSS as internal standard at room temperature. The mixture was immediately transferred to an NMR tube and the spectrum acquired at ~15 min after the start of the reaction.

Isolation of cycloadduct of 2 and *endo*-BCN-OH (4). Ac-TePhe-^{i}Pr (9.2 mg, 0.026 mmol, 1 eqv.) was suspended in 50 mM phosphate buffer, pH 7.0 (5.2 mL), to which was added NCS (8.9 mg, 0.067 mmol, 2.5 eqv.) and the mixture briefly sonicated until full dissolution was achieved. BCN (4.5 mg, 0.030 mmol, 1.2 eqv) was dissolved in 0.1 mL MeOH and added to the reaction mixture, resulting in immediate formation of a fine white precipitate presumed to be extruded oxidized Te. The reaction was mixed again by brief sonication and left to stand at room temp. for 30 min. Precipitates were removed by centrifugation at 21.1 x *g* for 15 min. The supernatant was diluted with H_2O (~1 mL) and extracted with DCM (4 x 4 mL). The combined organic phase was dried *in vacuo,* and dissolved in a minimal volume of MeOH for preparatory TLC (silica gel 60G F_{254}, 8% MeOH in DCM, product R_f = 0.5). Product was extracted from silica by repeated sonication in MeOH and centrifugation, followed by passage of the MeOH extract through a 0.45 μm PTFE syringe filter, and concentration *in vacuo* (5.7 mg white solid, 58% isolated; mixture of diastereomers). ^{1}H NMR (600 MHz, MeOD, 328 K) δ 7.04-6.94 (3 H, m, aryl H), 4.48 and 4.47 (1H, 2 overlapping t, J = 7.6 Hz, Hα), 3.87 and 3.86 (1H, 2 overlapping hept., J = 6.7 Hz, ^{i}Pr-C**H**$(CH_3)_2$), 3.69-3.58 (2H, m, HO-C**H₂**-cyclopropyl), 3.20-2.75 (6H, m, 2 Hβ and 4 cyclooctane benzylic H), 2.34-2.15 (2H, m, 2 cyclooctane homobenzylic H), 1.94 and 1.93 (3H, 2 s, *N*-Ac-C**H₃**), 1.48 (2H, broad s, 2 cyclooctane homobenzylic H), 1.07 (3H, 2 overlapping d, J = 6.6 Hz, ^{i}Pr-CH(C**H₃**)$_2$), 1.00 (1H, m, HO-CH_2-C**H**$(CH)_2$-) 0.92 (3H, 2 overlapping d, J = 6.6 Hz, ^{i}Pr-CH(C**H₃**)$_2$), 0.84 (2H, broad s, 2 bicyclo[6.1.0]nonane bridgehead H). ^{13}C NMR (125 MHz, MeOD, 298 K) δ 172.85, 172.82, 172.32, 172.27, 135.76, 130.96, 130.33, 129.37, 126.45, 126.42, 59.65, 59.60, 56.19, 42.45, 37.05, 35.20, 22.48, 22.47, 22.40, 22.38, 22.30. HR-MS: obs. 373.2485 ($[M+H]^+$), calc. 373.2486 (Fig. S6b).

Kinetics of OSTAC reaction monitored by UV-visible spectrophotometry. Measurements were carried out on UV-2401PC (Shimadzu) and Cintra 404 (GBC Scientific) spectrophotometers. The composition of solvent used to obtain all absorbance spectra and kinetic runs is phosphate buffer, 2 mM, pH 7, 5% D_2O and 10% MeOH in H_2O (D_2O results from preparation and quantification of Ac-TePhe-^{i}Pr stock solutions by NMR spectroscopy; MeOH to ensure full dissolution of BCN). Extinction coefficient determination for **2** and *endo*-BCN-OH at 323 nm is shown in Fig. S7a). For each kinetic run, **1**, NCS, buffer, and necessary volumes of D_2O/H_2O were pre-mixed to generate a solution of **2** (total volume 1800 uL), while *endo*-BCN-OH (in 200 μL MeOH) was deposited within a 10 mm quartz cuvette already seated in the spectrophotometer. Reaction was initiated by swiftly pipetting the mixture containing **2** down the side of the cuvette. Final reactant concentrations: **2** (50 μM), NCS (125, 200, or 400 μM total prior to oxidation of **1**), *endo*-BCN-OH (75 μM).

Reaction of 2 with DIBAC-OH. A solution of 1 (1.0 mM), DIBAC-OH (2.0 mM), and NCS (8 mM) was prepared in phosphate buffer, 50 mM, pD 7.4 + 10% MeOD + DSS at room temperature. The mixture was immediately transferred to an NMR tube and spectra acquired at 40 minute intervals. Acquisition time for each spectrum was approximately 25 min due to the long relaxation delay used (θ = 90 °, d1 = 40 sec); the midpoint of each acquisition was set to represent each time point in subsequent analyses. Formation of the hypothesized cycloadduct was supported by ESI-MS analysis (Fig. S8b).

OSTAC Labeling of TePhe S-peptide. TePhe S-peptide (500 μM) in PBS was incubated with NCS (1.5 mM, 3 eqv.) and *endo*-BCN-OH (1.0 mM, 2 eqv.) for 30 min. at room temp. at which point the reaction mixture was flash frozen in liquid nitrogen and stored at -80 °C. Immediately prior to analysis, a TePhe S-peptide control and the reaction mixture were thawed, diluted 1:3 with 2,5-dihydroxybenzoic acid matrix in 1:1 H_2O/ACN + 0.1% TFA, and applied to a MTP 384 ground steel target. Spectra were acquired on a Bruker Autoflex Speed MALDI-TOF mass spectrometer in reflectron mode.

Expression and purification of TePhe-containing proteins. MBP, Bcx, and $3CL^{pro}$ were recombinantly expressed in BL21 (DE3) *E. coli* using published procedures[22] in Phe-deficient M9 minimal media[56] supplemented with TePhe

(1 mM). MBP with C-terminal His-tag was purified by affinity chromatography. Bcx was purified by cation exchange. $3CL^{pro}$ was expressed as a GST-fusion, purified on glutathione-agarose, and the GST-tag cleaved using Factor Xa. Protein identity and purity were verified by SDS-PAGE and ESI-MS; concentrations were determined by BCA assay. Detailed procedures for protein expression and purification can be found in the Supporting Information.

Azidoacetylation of BSA. The NHS-ester of azidoacetic acid was generated by stirring together azidoacetic acid (6.0 mg, 59 μmol, 1 eqv.), EDC·HCl (11 mg, 57 μmol, 1 eqv.), *N*-hydroxy-succinimide (NHS, 6.5 mg, 56 μmol, 1 eqv.) in DMF (1.5 mL) at room temperature for 2 hr. BSA (Bioshop) was dissolved at 4 mg/mL in PBS (total volume 2 mL), to which was added 16.2 μL of the NHS-ester reaction (final [NHS-ester] = 300 μM, [BSA] = 60 μM) and the mixture incubated at room temp. for 2.5 hr. Purification and concentration of azidoacetylated BSA (Az-BSA) was achieved using a 10 kDa MWCO centrifugal unit.

General considerations for protein labeling reactions gel imaging. All labeling reactions were performed at room temperature in buffered solution with 0.2% SDS. Stock solutions of NCS (20 to 50 mM in H_2O) and iodoacetamide (100 to 500 mM in H_2O) were prepared immediately before use. Stock solutions of strained alkynes and strained alkyne-fluorophore conjugates were prepared in DMSO, stored at -20 °C, and diluted using H_2O immediately prior to addition to labeling reactions. Reaction volumes range from 10 to 25 μL. Reaction quenching was achieved using a large excess of non-fluorescent *endo*-BCN-OH (typically 1 mM). Unless otherwise stated, reaction mixtures were mixed directly with loading dye and subjected to standard SDS-PAGE analysis on 10, 12.5, or 15% gels. In-gel fluorescence was detected using a 465 nm blue LED and 525 nm filter (FAM) or a 520 nm green LED and 605 nm filter (TAMRA). Following fluorescence imaging, gels were stained with Coomassie Brilliant Blue to visualize all protein bands. Intensity of fluorescence and Coomassie staining was quantified using the GelAnalyzer software.

Oxidant concentration dependence of OSTAC labeling on MBP. Wt and TePhe MBP (1 mg/mL (24 μM) in 50 mM phosphate buffer, pH 7, 0.2% SDS) were treated with BCN-FAM (100 μM) and NCS (0, 0.25, 0.5, or 0.75 mM) or $NaIO_4$ (0, 2.5, 5.0, or 7.5 mM) for 1 hr.

Timecourse of OSTAC labeling on MBP. To a mixture of Wt or TePhe MBP (0.02 mg/mL (500 nM) in PBS + 0.2% SDS) and BCN-FAM (10 μM) was added NCS (20 μM) to initiate the reaction. At each timepoint, a small aliquot of the reaction mixture was quenched by rapid transfer into a solution of *endo*-BCN-OH (1 mM in DMSO, 10x volume of reaction aliquot). Colloidal Coomassie Brilliant Blue G (Sigma) was used to visualize the low protein concentrations used in this experiment.

Oxidant concentration dependence of OSTAC labeling on Bcx. Wt and TePhe Bcx (1 mg/mL (50 μM) in 50 mM phosphate buffer, pH 7, 0.2% SDS) were treated with BCN-FAM (100 μM) and NCS (0, 0.25, 0.5, 0.75 mM) for 5 min.

Competition between BCN and DIBAC for reaction with oxidized TePhe. To a mixture containing TePhe MBP (0.025 mg/mL (600 nM) in PBS + 0.2% SDS) and BCN-FAM (2.5 μM) was added DIBAC-TAMRA (0, 2.5, 12.5, 50, or 250 μM). NCS (20 μM) was added and labeling allowed to proceed for 15 min.

OSTAC labeling and blocking of non-specific binding on $3CL^{pro}$. Wt and TePhe $3CL^{pro}$ (0.5 mg/mL (15 μM) in PBS + 0.2% SDS) were subjected to 4 labeling conditions: unoxidized control (no NCS, 100 μM BCN-FAM), labeling without blocking (500 μM NCS, 100 μM BCN-FAM, 5 min), IAA blocking only (1 mM, 20 min) followed by labeling (500 μM NCS, 100 μM BCN-FAM, 5 min), or sequential IAA and DIBAC blocking (1 mM IAA, 20 min, then 100 μM DIBAC-OH and 250 μM NCS, 5 min) followed by labeling (250 μM NCS, 100 μM BCN-FAM, 5 min).

Blocking of non-specific proteome labeling. BL21 (DE3) *E. coli* lysate (1 mg/mL total protein in PBS + 0.2% SDS), alone or spiked with Wt or TePhe MBP (0.02 mg/mL) were subjected to BCN-FAM labeling with or without blocking with DIBAC-OH. Unblocked samples were labeled directly BCN-FAM (with 10 μM) and NCS (500 μM) for 5 min. Blocked samples were treated first with DIBAC-OH (100 μM) and NCS (500 μM) for 5 min, followed by addition of BCN-FAM (10 μM) for 5 min. A positive control for BCN-FAM-labeled MBP was generated by incubating TePhe MBP (0.1 mg/mL) with BCN-FAM (20 μM) and NCS (50 μM).

Selective in-lysate OSTAC labeling of TePhe MBP, Bcx, and 3CL^{pro}. BL21 (DE3) *E. coli* lysate (1 mg/mL total protein in PBS + 0.2% SDS) was spiked with Wt or TePhe MBP/Bcx/3CL^{pro} (0.01 mg/mL each). Lysates were alkylated with IAA (5 mM, 20 min), followed by blocking with DIBAC-OH (50 μM) and NCS (200 μM) for 5 min, and labeling with BCN-FAM (25 μM) and additional NCS NCS (100 μM) for 5 min. Purified protein controls (0.01 mg/mL each of MBP/Bcx/3CL^{pro}) were alkylated with IAA (5 mM, 20 min), blocked with DIBAC-OH (5 μM) and NCS (5 μM), and labeled with BCN-FAM (25 μM) and additional NCS (10 μM).

Search for intermolecular crosslinking during OSTAC. Wt and TePhe 3CL^{pro} was kept alone or mixed pairwise with each of Wt BSA, MBP, and Bcx (0.5 mg/mL per protein in PBS + 0.2% SDS). Each sample was alkylated with IAA (1 mM, 25 min) and divided into 2 aliquots. Control aliquots ("-" conditions) were incubated with BCN-FAM (150 μM), without NCS, for 5 min. Test aliquots ("+" conditions) were blocked with DIBAC-OH (150 μM) and NCS (375 μM) for 5 min, followed by labeling with BCN-FAM (150 μM) and additional NCS (375 μM) for 5 min.

Compatibility of OSTAC and SPAAC reactions. Az-BSA and TePhe MBP were mixed at 0.2 mg/mL each in PBS + 0.2% SDS and alkylated with IAA (1 mM, 15 min) prior to further labeling. Aliquots were then subjected to various conditions: no probe or oxidant for 1 hr, SPAAC with DIBAC-TAMRA only (100 μM) for 1 hr, SPAAC with BCN-FAM only (100 μM) for 1 hr, OSTAC with BCN-FAM (100 μM) and NCS (100 μM) for 1 hr, stepwise SPAAC and OSTAC with DIBAC-TAMRA (100 μM) first for 1 hr followed by BCN-FAM (25 μM) and NCS (100 μM) for 5 min, or simultaneous SPAAC and OSTAC with DIBAC-TAMRA (250 μM), BCN-FAM (25 μM) and NCS (100 μM) for 1 hr.

Compatibility of OSTAC and CuAAC reactions. Az-BSA was kept alone or mixed with all Wt or all TePhe combinations of MBP, Bcx, and 3 CL^{pro} in PBS + 0.2% SDS (100 μL per sample). Samples were alkylated with IAA (2 mM, 20 min). CuAAC was performed by addition of $CuSO_4$ (0.5 mM), THPTA (2.5 mM), alkyne-TAMRA (0.1 mM), and sodium ascorbate (50 mM). After 1.5 hr, samples were repeatedly buffer exchanged in PBS + 0.2% SDS using 10 kDa MWCO centrifugal units (removal of ascorbate and Cu appears to have been successful but for unknown reasons all alkyne-TAMRA was retained with the protein mixture). The retentate volume was readjusted to 100 μL; half of each sample was saved for analysis while half was subjected to OSTAC conditions. OSTAC samples (post-CuAAC as well as control consisting only of TePhe MBP, Bcx, 3Cl^{pro}) were blocked with DIBAC-OH (100 μM) and NCS (200 μM) for 5 min, followed by labeling with BCN-FAM (100 μM) and additional NCS (200 μM) for 5 min.

Acknowledgments
The authors would like to thank Dr. Darcy Burns, Dr. Jack Sheng, and Dr. Karl Demmans at the University of Toronto CSI-COMP NMR Facility for their help in spectra acquisition and interpretation; Dr. Matthew Forbes and Dr. Chung Woo Fung at the University of Toronto Advanced Instrumentation for Molecular Structure (AIMS) Facility for mass spectra acquisition; and Prof. Lisa Willis (University of Alberta) for generation of plasmids used for this project. The authors are also grateful to Prof. Andrew Woolley and Prof. Voula Kanelis of the University of Toronto chemistry department for insightful discussions, and Prof. Anthony Rullo (McMaster University) for comments on the manuscript. Y.J.B. is a recipient of NSERC CGS-D and the University of Toronto Faculty of Arts and Sciences Top Doctoral Fellowship. This project is further funded by the Natural Science and Engineering Research Council (NSERC) through a Discovery Grant to M.N.

References

1. Kovalski, J. R.; Kuzuoglu-Ozturk, D.; Ruggero, D. Protein Synthesis Control in Cancer: Selectivity and Therapeutic Targeting. *EMBO J.* **2022,** *41,* e109823.

2. Skariah, G.; Todd, P. K. Translational Control in Aging and Neurodegeneration. *Wiley Interdiscip. Rev. RNA* **2021,** *12*, e1628.

3. Scheper, G. C.; van der Knaap, M. S.; Proud, C. G. Translation Matters: Protein Synthesis Defects in Inherited Disease. *Nat. Rev. Genet.* **2007,** *8,* 711-723.

4. Dermit, M.; Dodel, M.; Mardakheh, F. K. Methods for Monitoring Measurement of Protein Translation in Time and Space. *Mol. BioSyst.* **2017,** *13,* 2477-2488.

5. Iwasaki, S.; Ingolia, N. T. The Growing Toolbox for Protein Synthesis Studies. *Trends Biochem. Sci.* **2017,** *42*, 612-624.

6. Saleh, A. M.; Wilding, K. M.; Calve, S.; Bundy, B. C.; Kinzer-Ursem, T. L. Non-canonical Amino Acid Labeling in Proteomics and Biotechnology. *J. Biol. Eng.* **2019,** *13,* 43.

7. van Bergen, W.; Heck, A. J. R.; Baggelaar, M. P. Recent Advancements in Mass Spectrometry–based Tools to Investigate Newly Synthesized Proteins. *Curr. Opin. Chem. Biol.* **2022,** *66,* 102074.

8. Bassan, J.; Willis, L. M.; Vellanki, R. N.; Nguyen, A.; Edgar, L. J.; Wouters, B. G.; Nitz, M. TePhe, a Tellurium-containing Phenylalanine Mimic, Allows Monitoring of Protein Synthesis In Vivo with Mass Cytometry. *Proc. Natl. Acad. Sci.* **2019,** *116*, 8155-8160.

9. a) Sletten, E.; Bertozzi, C. Bioorthogonal Chemistry: Fishing for Selectivity in a Sea of Functionality. *Angew. Chem. Int. Ed.* **2009,** *48*, 6974-6998.
b) McKay, C.; Finn, M. G. Click Chemistry in Complex Mixtures: Bioorthogonal Bioconjugation. *Chem. Biol.* **2014,** *21*, 1075-1101.

10. a) Wu, D.; Yang, K.; Zhang, Z.; Feng, Y.; Rao, L.; Chen, X.; Yu, G. Metal-free Bioorthogonal Click Chemistry in Cancer Theranostics. *Chem. Soc. Rev.* **2022,** *51*, 1336-1376.
b) Deb, T.; Tu, J.; Franzini, R. Mechanisms and Substituent Effects of Metal-Free Bioorthogonal Reactions. *Chem. Rev.* **2021,** *121*, 6850-6914.
c) Bird, R.; Lemmel, S.; Yu, X.; Zhou, Q. Bioorthogonal Chemistry and Its Applications. *Bioconjug. Chem.* **2021,** *32*, 2457-2479.

11. Nguyen, S. S.; Prescher, J. A. Developing Bioorthogonal Probes to Span a Spectrum of Reactivities. *Nat. Rev. Chem.* **2020,** *4,* 476-489.

12. Hu, Y.; Schomaker, J. Recent Developments and Strategies for Mutually Orthogonal Bioorthogonal Reactions. *ChemBioChem.* **2021,** *22*, 3254-3262.

13. Dieterich, D. C.; Link, A. J.; Graumann, J.; Tirrell, D. A.; Schuman, E. M. Selective Identification of Newly Synthesized Proteins in Mammalian Cells Using Bioorthogonal Noncanonical Amino Acid Tagging (BONCAT). *Proc. Natl. Acad. Sci.* **2006,** *103*, 9482-9487.

14. Elliot, T. S.; Bianco, A.; Townsley, F. M.; Fried, S. D.; Chin, J. W. Tagging and Enriching Proteins Enables Cell-specific Proteomics. *Cell Chem. Biol.* **2016,** *23*, 805-815.

15. Mahdavi, A.; Hamblin, G. D.; Jinda, G. A.; Bagert, J. D.; Dong, C.; Sweredoski, M. J.; Hess, S.; Schuman, E. M.; Tirrell, D. A. Engineered Aminoacyl-tRNA Synthetase for Cell-selective analysis of Mammalian protein synthesis. *J. Am. Chem. Soc.* **2016,** *138*, 4278–4281.

16. Aviner, R.; Geiger, T.; Elroy-Stein, O. Novel Proteomic Approach (PUNCH-P) Reveals Cell Cycle-specific Fluctuations in mRNA Translation. *Genes Dev.* **2013**, *27*, 1834–1844.

17. Forester, C. M.; Zhao, Q.; Phillips, N. J.; Urisman, A.; Chalkley, R. J.; Oses-Prieto, J. A.; Zhang, L.; Ruggero, D.; Burlingame, A. L. Revealing Nascent Proteomics in Signaling Pathways and Cell Differentiation. *Proc. Natl. Acad. Sci.* **2018,** *115*, 2353-2358.

18. Tong, M.; Suttapitugsakul, S.; Wu, R. Effective Method for Accurate and Sensitive Quantitation of Rapid Changes of Newly Synthesized Proteins. *Anal. Chem.* **2020,** *92*, 10048-10057.

19. Kiick, K. L.; Saxon, E.; Tirrell, D. A.; Bertozzi, C. R. Incorporation of Azides into Recombinant Proteins for Chemoselective Modification by the Staudinger Ligation. *Proc. Natl. Acad. Sci.* **2001,** *99*, 19-24.

20. Marciano, R.; Leprivier, G.; Rotblat, B. Puromycin Labeling Does Not Allow Protein Synthesis to be Measured in Energy-starved Cells. *Cell Death Dis.* **2018**, *9*, 4–6.

21. Aviner, R. The Science of Puromycin: From Studies of Ribosome Function to Applications in Biotechnology. *Comput. Struct. Biotechnol. J.* **2020,** *18,* 1074-1083.

22. Bu, Y. J.; Nitz, M. Incorporation of TePhe into Expressed Proteins is Minimally Perturbing. *ChemBioChem.* **2021,** *22*, 2449-2456.

23. Vurgun, N.; Nitz, M. Validation of L-Tellurienylalanine as a Phenylalanine Isostere. *ChemBioChem.* **2020,** *21*, 1136-1139.

24. Brüne, D.; Andrade-Navarro, M. A.; Mier, P. Proteome-wide Comparison between the Amino Acid Composition of Domains and Linkers. *BMC Res. Notes* **2018,** *11,* 117.

25. McCormick, T. M.; Jahnke, A. A.; Lough, A. J.; Seferos, D. S. Tellurophenes with Delocalized π-Systems and Their Extended Valence Adducts. *J. Am. Chem. Soc.* **2012,** *134,* 3542-3548.

26. Carrera, E. I.; Seferos, D. S. Efficient halogen Photoelimination from Dibromo, Dichloro and Difluoro Tellurophenes. *Dalton Trans.* **2015,** *44,* 2092–2096.

27. Carrera, E. I.; Seferos, D. S. Ring Opening of π-Delocalized 2,5-Diphenyltellurophene by Chemical or Self-Sensitized Aerobic Photooxidation. *Organometallics* **2017,** *36*, 2612-2621.

28. McCormick, T. M.; Carrera, E. I.; Schona, T. B.; Seferos, D. S. Reversible Oxidation of a Water-soluble Tellurophene. *Chem. Commun.* **2013,** *49*, 11182-11184.

29. Umezawa, T.; Sugihara, Y.; Ishii, A.; Nakayama, J. Synthesis and Properties of Monicyclic Selenophene 1-Oxides. *J. Am. Chem. Soc.* **1998,** *120*, 12351-12352.

30. Detty, M. R. Reaction Pathways of Telluroxide Equivalents. Reductive Elimination of Hydrogen Peroxide from Dihydroxytelluranes and Oxidation of Carbon via Intramolecular Transfer of Oxygen. *Organometallics* **1991,** *10,* 702-712.

31. Detty, M. R. Oxidation of Selenides and Tellurides with Positive Halogenating Species. *J. Org. Chem.* **1980,** *45,* 274-279.

32. Engman, L.; Lind, J.; Merényi , G. Redox Properties of Diaryl Chalcogenides and Their Oxides. *J. Phys. Chem.* **1994,** *98,* 3174-3182

33. You, Y.; Ahsan, K.; Detty, M. R. Mechanistic Studies of the Tellurium(II)/Tellurium(IV) Redox Cycle in Thiol Peroxidase-like Reactions of Diorganotellurides in Methanol. *J. Am. Chem. Soc.* **2003,** *125*, 4918–4927

34. Melles, J.; Backer, H. J. Sesquioxydes Obtenus par Oxydation de Thiophenes: (Propriétés du Groupe Sulfonyle XXXVI). *Recl. Trav. Chim. Pays-Bas* **1953,** *72,* 491-496.

35. van Tilborg, W. J. M. Improved Method for the Synthesis of Dialkyl-substituted Thiophene 1,1-dioxides. *Synth. Commun.* **1976**, *6*, 583-589

36. Li, Y. Q; Thiemann, T.; Sawada, T.; Mataka, S; Tashiro, M. Lewis Acid Catalysis in the Oxidative Cycloaddition of Thiophenes. *J. Org. Chem*. **1997**, *62*, 7926-7936.

37. Meguro, T.; Yoshida, S.; Hosoya, T. Sequential Molecular Conjugation Using Thiophene S,S-Dioxides Bearing a Clickable Functional Group. *Chem. Lett.* **2017,** *46*, 1137-1140.

38. Wang, W.; Ji, X.; Dua, Z.; Wang, B. Sulfur Dioxide Prodrugs: Triggered Release of SO_2 via a Click Reaction. *Chem. Commun.* **2017,** *53*, 1370-1373.

39. Nakayama, J.; Yamaoka, S.; Nakanishi, T.; Hoshino, M. 3,4-Di-tert-butylthiophene 1,1-dioxide, a Convenient Precursor of *o*-Di-tert-butylbenzene and Its Derivatives. *J. Am. Chem. Soc.* **1988,** *110*, 6598–6599.

40. Detty, M. R.; Friedman, A. E. Oxidation of Tellurapyrylium Dyes with Ozone, Chlorine, and Bromine. Differing Regiochemical and Kinetic Behavior with Respect to Oxidations of Oxygen-, Sulfur-, and Selenium-Containing Dyes. *Organometallics* **1994,** *13*, 533-540.

41. MacKenzie, D. A.; Sherratt, A. R.; Chigrinova, M.; Cheung, L. L. W.; Pezacki, J. P. Strain-promoted Cycloadditions Involving Nitrones and Alkynes — Rapid Tunable Reactions for Bioorthogonal Labeling. *Curr. Opin. Chem. Biol.* **2014,** *21*, 81-88.

42. Hong, V.; Presolski, S. I.; Ma, C.; Finn, M. G. Analysis and Optimization of Copper-Catalyzed Azide–Alkyne Cycloaddition for Bioconjugation. *Angew. Chem. Int. Ed.* **2009**, *48*, 9879–9883.

43. Hein, J. E.; Fokin, V. V. Copper-catalyzed Azide–alkyne Cycloaddition (CuAAC) and Beyond: New Reactivity of Copper(I) Acetylides. *Chem. Soc. Rev.* **2010**, *39*, 1302–1315.

44. Dommerholt, J.; Rutjes, F. P. J. T.; van Delft, F. L. Strain-Promoted 1,3-Dipolar Cycloaddition of Cycloalkynes and Organic Azides. *Top. Curr. Chem.* **2016,** *374*, 16.

45. Karver, M. R.; Weissleder, R.; Hilderbrand, S. A. Bioorthogonal Reaction Pairs Enable Simultaneous, Selective, Multi-Target Imaging. *Angew. Chem. Int. Ed.* **2011,** *51*, 920-922.

46. Borrmann, A.; Fatunsin, O.; Dommerholt, J.; Jonker, A. M.; Löwik, D. W. P. M.; van Hest, J. C. M.; van Delft, F. L. Strain-Promoted Oxidation-Controlled Cyclooctyne−1,2-Quinone Cycloaddition (SPOCQ) for Fast and Activatable Protein Conjugation. *Bioconjug. Chem.* **2015,** *26*, 257–261.

47. van Beek, H. C. A.; Hendriks, C. H. F.; van der Net, G. J.; Schaper, L. Reversible Halogenation of Cyanine Dyes. *Recl. Trav. Chim. Pays-Bas* **1975,** *94,* 31-34.

48. Geoghegan, K. F.; Stroh, J. G. Site-directed Conjugation of Nonpeptide Groups to Peptides and Proteins via Periodate Oxidation of a 2-amino Alcohol. Application to Modification at N-terminal Serine. *Bioconjug. Chem.* **1992,** *3*, 138-146.

49. Agarwal, P.; van der Weijden, J.; Sletten, E. M.; Rabuka, D.; Bertozzi, C. R. A Pictet-Spengler Ligation for Protein Chemical Modification. *Proc. Natl. Acad. Sci.* **2012,** *110*, 46-51.

50. Brabham, R. L.; Keenan, T.; Husken, A.; Bilsborrow, J.; McBerney, R.; Kumar, V.; Turnbull, W. B.; Fascione, M. A. Rapid Sodium Periodate Cleavage of an Unnatural Amino Acid Enables Unmasking of a Highly Reactive α-oxo Aldehyde for Protein Bioconjugation. *Org. Biomol. Chem*. **2020,** *18*, 4000-4003.

51. van Geel, R.; Pruijn, G. J. M.; van Delft, F. L.; Boelens, W. C. Preventing Thiol-Yne Addition Improves the Specificity of Strain-Promoted Azide–Alkyne Cycloaddition. *Bioconjug. Chem.* **2012,** *23*, 392–398.

52. Dommerholt, J.; van Rooijen, O.; Borrmann, A.; Guerra, C. F.; Bickelhaupt, F. M.; van Delft, F. L. Highly Accelerated Inverse Electron-demand Cycloaddition of Electron-deficient Azides with Aliphatic Cyclooctynes. *Nat. Commun.* **2014,** *5,* 5378.

53. Quiocho, F. A.; Spurlino, J. C.; Rodseth, L.E. Extensive Features of Tight Oligosaccharide Binding Revealed in High-resolution Structures of the Maltodextrin Transport/Chemosensory Receptor. *Structure* **1997,** *5,* 997-1015.

54. Wakarchuk, W. W.; Campbell, R. L.; Sung, W. L.; Davoodi, J.; Yaguchi, M. Mutational and Crystallographic Analyses of the Active Site Residues of the Bacillus Circulans Xylanase. *Protein Sci.* **1994,** *3,* 467-475.

55. Iketani, S.; Forouhar, F.; Liu, H.; Hong, S. J.; Lin, F. Y.; Nair, M. S.; Zask, A.; Huang, Y.; Xing, L.; Stockwell, B. R.; Chavez, A.; Ho, D. D. Lead Compounds for the Development of SARS-CoV-2 3CL Protease Inhibitors. *Nat. Commun.* **2021**, *12*, 2016.

56. Rathod, R.; Kang, Z.; Hartson, S. D.; Kumauchi, M.; Xie, A.; Hoff, W. D. Side-chain Specific Isotopic Labeling of Proteins for Infrared Structural Biology: The Case of Ring-d-4-tyrosine Isotope Labeling of Photoactive Yellow Protein. *Protein Expr. Purif.* **2012,** *85*, 125-132.